SUPPLEMENTAL DATA

SUPPLEMENTAL FIGURE LEGENDS

Figure S1, related to Figure 1. Wnt reporter expression and analysis of β-catenin deletion and ectopic expression of *Dkk1* and *Krm1*. (A-D) X-gal stained paraffin sections of dorsal skin from *Axin2*^{lacZ} mice 3 days after hair plucking at P54 to induce anagen (A,C); at 1 year of age in the absence of hair plucking (early anagen) (B); or at 5 months in the absence of hair plucking (telogen) (D). Sections in (A,C,D) were counterstained with nuclear fast red. Blue signal indicating *Axin2*^{lacZ} expression is observed in the IFE (B,D) and in DP, SHG, matrix, and hair shaft (HS) precursors in anagen HF (A-C). Expression is absent from the HF DP, SHG and bulge in telogen but present in HF epithelia above the bulge (D). (E-H) Frozen sections of dorsal skin from *TCF/Lef:H2B-GFP* (*TL-GFP*) mice at P21 (E) (early anagen), P10 (F,G) (mid-anagen) and P20 (H) (telogen) photographed under fluorescence illumination to visualize GFP (green). Reporter expression is observed in the IFE, more broadly at P20 (H) and P21 (E) than at P10 (F), as well as in DP, matrix and hair shaft (HS) precursor cells in anagen HF (E,G). In telogen (H), expression is seen in the upper HF, but not in the DP, bulge or SHG. (I,J) X-gal stained frozen sections of dorsal tongue epithelium (I) and footpad skin (J) from *Axin2*^{lacZ} mice at 1 year of age. The reporter is expressed at the base of tongue filiform papillae (FiP) (I) and in basal epidermis and underlying dermal cells of the footpad (J). (K,L) Frozen sections of *TCF/Lef:H2B-GFP* dorsal tongue (K) and footpad (L) at 5 months of age. GFP expression is detected in epithelial basal cells of tongue filiform papillae that also express the basal marker KRT14, and in some suprabasal cells (K). In adult footpad skin (L), GFP is detected in cells of the upper

dermis but is largely absent from the epithelium. (M,N) In situ hybridization of dorsal skin at P23 using ^{35}S-labeled probes for *Wnt3* (M) and *Wnt10a* (N). Sections are photographed under red illumination to reveal silver grains. *Wnt3* is expressed in IFE (M), and *Wnt10a* in IFE and in the DP and SHG of early anagen HF (N). Sections in (E-H) and (K-N) are DAPI-counterstained (blue) to reveal nuclei. Arrows indicate positive signals. (O) PCR analysis of genomic DNA isolated from dorsal epidermis (epi) and dermis (der) of doxycycline-treated *Krt5-rtTA tetO-Cre Ctnnb1$^{fl/fl}$* and control *Krt5-rtTA Ctnnb1$^{fl/+}$* mice. PCR products of 221bp (wild type allele) and 324bp (floxed allele) are detected in *Krt5-rtTA Ctnnb1$^{fl/+}$* DNA. The floxed recombined (knockout) allele (500bp PCR product) is prominent in *Krt5-rtTA tetO-Cre Ctnnb$^{fl/fl}$* epidermal DNA. The floxed (non-recombined) allele is also detected indicating that deletion is not 100% efficient. The knockout allele is weakly detected in dermal DNA, likely reflecting presence of hair follicle remnants in the isolate. (P,Q) Immunohistochemistry for β-catenin (brown) confirms deletion of β-catenin protein in doxycycline-induced *Krt5-rtTA tetO-Cre Ctnnb1$^{fl/fl}$* skin epithelial cells. (R,S) In situ hybridization for *Dkk1* (purple-brown) shows the presence of *Dkk1* expression in doxycycline-induced *Krt5-rtTA tetO-Dkk1* skin (S) compared with uninduced skin (R). (T) Semi-quantitative RT-PCR analysis of wild-type dorsal skin at different hair cycle stages using 28 amplification cycles. (U) qPCR analysis of *Krm1* at successive hair cycle stages in wild-type skin, normalized to *GAPDH* levels. Results are shown as mean ± SEM. One way ANOVA was conducted using IGOR Pro (WaveMetrics Inc., Lake Oswego, OR) and p-values calculated using the Tukey test. *Krm1* levels appear elevated in late anagen, but this does not reach statistical significance. (V) Semi-quantitative RT-PCR analysis of reverse-transcribed total RNA from dorsal skin using primers specific for mouse *Krm1* and 24 cycles of amplification. *GAPDH* was amplified as a control. PCR was performed with RNA samples processed with (+) or without (-) reverse transcriptase. Expression of *Krm1* is detected at low levels

in *Krt5-rtTA* control skin and is markedly elevated in *Krt5-rtTA KRT14-Krm1* skin. (W,X) Histological analysis reveals absence of gross changes resulting from expression of *Kremen1* in P14 *KRT14-Krm1 Krt5-rtTA* transgenic skin (X) compared with *Krt5-rtTA* control littermate skin (W). Scale bars: 50μm (A-C,F,P,Q), 100μm (D,E,G-I,K-N,R,S), and 200μm (J,W,X).

Figure S2, related to Figures 2-5. Effects of *Dkk1* expression or deletion of β-catenin or *Wls* on HF growth, proliferation and stem cell maintenance. (A) Quantification of BrdU positive nuclei as a percent of the total number of DAPI-labeled nuclei in hair bulbs of control mice (n=2) and *Dkk1*-expressing mice (n=2). Mice were doxycycline treated from P4 and analyzed at P8. Nuclei in a total of 17 control hair bulbs and 13 *Dkk1* transgenic hair bulbs were counted. Results are presented as mean ± SEM. (B-E) Immunofluorescence for BrdU (B,C, red, arrows) and immunohistochemistry for cyclin D1 (D,E, brown, arrows) in skin sections of control and *Krt5-rtTA tetO-Dkk1* double transgenic mice doxycycline treated from P4 and analyzed at P8. (F,G) Immunohistochemistry for cyclin D1 (brown, arrows) in skin sections of control and *Krt5-rtTA tetO-Cre Ctnnb1*$^{fl/fl}$ mutant mice doxycycline treated from P4 and analyzed at P8. Dark brown/black coloration in (F,G) is due to hair shaft pigmentation. (H-K) *Krt5-rtTA tetO-Cre Ctnnb1*$^{fl/fl}$ mice and control littermates were induced from P17 and dorsal skin was harvested at P25 (H,I) or P30 (J,K). β-catenin deletion in *Krt5-rtTA tetO-Cre Ctnnb1*$^{fl/fl}$ mice causes failure of natural anagen onset (I,K). (L,M) *Krt15-CrePR1 Ctnnb1*$^{fl/fl}$ and control mice were induced for 5 days prior to plucking at P54 and skin was harvested at P59. Co-immunofluorescence for CD34 (green, yellow arrows) and β-catenin (red) reveals β-catenin deletion in bulge stem cells in *Krt15-CrePR1 Ctnnb1*$^{fl/fl}$ mutant HFs but its persistence in IFE and HF regions above the bulge (M). Insets in

(L,M) represent higher magnification photographs of regions indicated by arrows. (N) Littermate control and *Krt15-CrePR1 Ctnnb1*$^{fl/fl}$ mice were treated topically with 1% mifepristone for 5 days prior to plucking at P54, and were photographed at P68. Robust hair re-growth was observed in control, but not *Krt15-CrePR1 Ctnnb1*$^{fl/fl}$ mutant mice. (O,P) *Krt5-rtTA tetO-Cre Wls*$^{fl/fl}$ and control mice were doxycycline treated from P4-P18. Immunohistochemistry (brown) confirms efficient deletion of Wls in doxycycline-induced *Krt5-rtTA tetO-Cre Wls*$^{fl/fl}$ skin epithelia analyzed at P60. (Q,R) *Krt15-CrePR1 Wls*$^{fl/fl}$ mice and control littermates were treated topically with 1% mifepristone from P19-P25 and analyzed at P60. Wls immunofluorescence (red) reveals absence of Wls protein in the bulge (R, arrow) and SHG of hair follicles in *Krt15-CrePR1 Wls*$^{fl/fl}$ mutant HF and its persistence in HF epithelia above the bulge and IFE. (S-X) *Krt5-rtTA tetO-Cre Wls*$^{fl/fl}$ mice were doxycycline treated from P4 and analyzed at P14. *Wls* mutant HF regress prematurely (S,T). Immunofluorescence (green) for Ki67 (U,V) and KRT15 (W,X) reveals absence of proliferation and persistence of bulge stem cells in *Wls* mutant HFs. Scale bars: 50μm (B-G,L,M,O-R,U-X); 100μm (H-K,S,T).

Figure S3, related to Figures 3 and 4. Ectopic *Dkk1* blocks plucking-induced and natural anagen.

(A,B) *Dkk1* transgenic and control littermate mice were doxycycline treated from P18 and hair was plucked at P52 to induce anagen. Immunohistochemistry for β-catenin (brown) revealed nuclear localized β-catenin in the matrix (black arrow) and DP (red arrow) of control HFs 5 days post-plucking (A). Nuclear β-catenin was severely reduced in the matrix, but still present in the DP (red arrow), of *Dkk1*-expressing HFs (B). (C-N) Double transgenic *Dkk1* and control littermate mice were doxycycline treated from P51, hair plucking was performed at P54, and mice were sacrificed 3 days post-plucking.

(C,D) Immunohistochemistry for cyclin D1 (brown, arrows) reveals reduced expression of cyclin D1 in *Dkk1* transgenic HF (D) compared with control (C). (E-H) Skin sections from doxycycline treated *Axin2*^{lacZ} Wnt reporter control (E,G) and *K5-rtTA tetO-Dkk1 Axin2*^{lacZ} (F,H) mice X-gal stained to visualize Wnt signaling activity (blue). Wnt reporter expression is detected in the DP (red arrow) and matrix and precortical cells (black arrows) of control hair follicles (E,G). In *Dkk1*-expressing follicles, reporter gene expression is detected in the DP (red arrows) but is reduced in epithelial cells (F,H). (I-N) Skin sections immunostained for pSmad1/5/8 (I,J, red), GATA3 (K,L, green) or AE13 (M,N, green) reveal expression of these markers in control hair follicles (I,K,M) and their absence in *Dkk1*-expressing follicles (J,L,N). Yellow arrows indicate positive signals in control hair follicles. (O-T) *Dkk1* and *Dkk1/Krm1* transgenic mice and control littermates were doxycycline treated from P17 and dorsal skin samples harvested at P25 (O-Q) or P30 (R-T). Expression of *Dkk1* alone (P,S) causes arrest of natural anagen compared with controls (O,R) and this occurs at an earlier stage in mice co-expressing *Dkk1* and *Krm1* (Q,T). Scale bars: 25μm (E,F); 50μm (A-D,G-N); 100μm (O-T).

Figure S4, related to Figure 5. Long-term broad deletion of epithelial β-catenin, but not ectopic expression of *Dkk1/Krm1*, results in HF loss and disappearance of stem cells.

Krt5-rtTA tetO-Cre Ctnnb1$^{fl/fl}$ mice and control littermates were doxycycline treated from P30; *Krt5-rtTA tetO-Dkk1* and *Krt14-Krm1 Krt5-rtTA tetO-Dkk1* transgenics and control littermates were doxycycline treated from P1. Mice were photographed at P100-102 and skin samples analyzed at the stages indicated. (A-E) *Krt5-rtTA tetO-Cre Ctnnb1*$^{fl/fl}$ (B) and *Krt14-Krm1 Krt5-rtTA tetO-Dkk1* (E) mice completely lack external hair, and *Krt5-rtTA tetO-Dkk1* double transgenics (D) show pronounced failure of hair growth compared with controls (A,C). H&E staining at P100-P102 (A'-E',U,V) or P180-P185 (K-O) reveals

the presence of HF structures in control (A',C',K,M,U), *Dkk1* transgenic (D',N) and *Dkk1*/*Krm1* transgenic (E',O) skin (arrows), although *Dkk1* transgenic and *Dkk1*/*Krm1* triple transgenic HFs show some structural abnormalities by P185 (M-O). In β-catenin mutants, the epidermis is thickened at P100 (B'); HF degrade and often form utricles (V), and are mostly absent by P180 (L) (arrows). Immunofluorescence for KRT15 (F,G, red; H-J,P-T, green) and CD34 (F',G',P'Q', red; H'-J',R'-T' green) (yellow arrows) reveals persistence of HF bulge stem cells in *Dkk1* transgenic (I,I',S,S') and *Dkk1*/*Krm1* transgenic (J,J',T,T') skin, and their absence in β-catenin mutant skin (G,G',Q,Q') at P100-P102 and P180-P185. (W,X) Alkaline phosphatase (AP) staining (blue; indicated by red arrows) shows dermal papillae associated with normal telogen HF in control P180 skin (W, red arrow), and at the tail end of a strand of degenerating HF epithelial cells in β-catenin mutant skin (X). Scale bars: 50μm (F-J',P-T') and 100μm (A'-E',K-O,U-X).

Figure S5, related to Figure 6. *Dkk1*-mediated inhibition of hair growth is reversible in mice expressing elevated *Kremen1*. Mice were placed on doxycycline at P1; doxycycline was withdrawn at P100. Skin biopsies were taken at P100 prior to doxycycline withdrawal (on Dox; A-Q) and at P115, 15 days after doxycycline withdrawal (off Dox; A'-Q'). (A-C,A'-C') Histological analysis shows that control hair follicles are in telogen, before and after doxycycline removal (A,A'). *Krt5-rtTA tetO-Dkk1* (DTG) and *KRT14-Krm1 Krt5-rtTA tetO-Dkk1* (TTG) hair follicles are arrested in very early anagen prior to doxycycline withdrawal (B,C); following doxycycline withdrawal these follicles spontaneously progress to full anagen (B',C'). Immunofluorescence (green) for KRT15 (D-F,D'-F') or CD34 (G-I,G'-I') reveals the presence of bulge stem cells in control, DTG and TTG hair follicles both before (D-I) and after (D'-I') doxycycline withdrawal (yellow arrows). (J-M,J'-M') Immunohistochemistry (brown) reveals absence of nuclear localized

β-catenin (J,K) and cyclin D1 (L,M) in DTG and TTG hair follicles on doxycycline, and presence of nuclear localized β-catenin and cyclin D1 in the matrix regions of DTG and TTG follicles following doxycycline withdrawal (J',K',L',M'; arrows). (N-Q,N'-Q') Immunofluorescence (green) for Ki67 (N,N',O,O') and AE13 (P,P',Q,Q') reveals absence of proliferation and hair shaft differentiation in DTG and TTG hair follicles prior to doxycycline withdrawal (N-Q), and the presence of proliferating matrix cells and differentiating hair shaft precursor cells following doxycycline withdrawal (N'-Q'; yellow arrows). Scale bars: 400μm (A-C,A'-C'); 100μm (E',F',H',I',L,M,L',M'); 50μm (D-K,D',G',J',K',N-Q,N'-Q').

Figure S6, related to Figures 5 and 7. Epidermal thickening following broad epithelial deletion of β-catenin or *Wls* is associated with hyperproliferation. (A) Littermate control and *Krt14-CreER Ctnnb1*$^{fl/fl}$ mice were treated topically with tamoxifen during the first telogen. (B) *Dkk1 Krm1* triple transgenic and control littermates were doxycycline treated from P4-P60. (C) *Krt5-rtTA tetO-Cre Wls*$^{fl/fl}$ and control mice were doxycycline treated from P4-P18. (D) *Krt15-CrePR1 Ctnnb1*$^{fl/fl}$ mice and control littermates were treated topically with 1% mifepristone from P20-P27. (E) *Krt15-CrePR1 Wls*$^{fl/fl}$ and control littermates were treated topically with 1% mifepristone from P19-P25. All skin samples were harvested at P60 and subjected to immunostaining for Ki67 (red or green); p63 (red); KRT10 (green); KRT6 (green); KRT17 (green); or β-catenin (brown), as indicated. Genotypes are indicated on the left; littermate controls are shown above each row of mutant photomicrographs. Arrows indicate positive signals. Epidermis in *Krt14-CreER Ctnnb1*$^{fl/fl}$ and *Krt5-rtTA tetO-Cre Wls*$^{fl/fl}$ mutants shows dramatically increased proliferation, expanded expression of the basal marker p63 and the suprabasal marker KRT10 and expression of the hyperproliferation markers KRT6 and

KRT17 (A,C). These phenotypes are not observed in mice expressing *Dkk1/Krm1* (B) or following *Krt15* promoter-driven deletion of β-catenin (D) or *Wls* (E) specifically in bulge and SHG cells. Scale bars: 50 μm.

Figure S7, related to Figures 5 and 7. Effects of broad deletion of epithelial β-catenin or *Wls* on skin ultrastructure and inflammation, and targeting scheme for insertion of *CreERT2tdT* cDNA into the endogenous *Axin2* locus. (A-D) Immunofluorescence (red) for α-catenin (A,B) or E-cadherin (C,D) shows the presence of both proteins at cell membranes in epidermis of control and *Krt5-rtTA tetO-Cre Ctnnb1*$^{fl/fl}$ mutant mice doxycycline treated from P4 and analyzed at P60. (E-J) *Krt5-rtTA tetO-Cre Ctnnb1*$^{fl/fl}$ mice, *Krt14-Krm1 Krt5-rtTA tetO-Dkk1* and littermate controls were doxycycline treated from P4-P60; *Krt5-rtTA tetO-Cre Wls*$^{fl/fl}$ mutants and littermate controls were doxycycline treated from P4-P18. All samples were analyzed at P60. Transmission electron microscopy of *Krt5-rtTA tetO-Cre Ctnnb1*$^{fl/fl}$ mutant (F) or *Krt5-rtTA tetO-Cre Wls*$^{fl/fl}$ mutant (J) epidermis reveals enlargement of intercellular spaces (yellow arrows) and cell membrane protrusions (white arrows) in some areas of mutant skin compared with controls (E,I). *Dkk1 Krm1* triple transgenic (H) epidermis shows normal cell membrane and desmosome presence compared with control (G). (K-T) Control littermates and *Krt14-CreER Ctnnb1*$^{fl/fl}$ mutants (K,L), *Krt15-CrePR1 Ctnnb1*$^{fl/fl}$ mutants (M,N), *Dkk1*/*Krm1* triple transgenics (O,P), *Krt5-rtTA tetO-Cre Wls*$^{fl/fl}$ mutants (Q,R) and *Krt15-CrePR1 Wls*$^{fl/fl}$ (S,T) were induced as described in the legend to Fig. S6 and paraffin sections were stained at P60 with Toluidine Blue O to detect mast cells. *Krt14-CreER Ctnnb1*$^{fl/fl}$ (L) and *Krt5-rtTA tetO-Cre Wls*$^{fl/fl}$ (R) mutants showed obvious increases in numbers of mast cells in the dermis compared with controls (K,Q). *Krt15-CrePR1 Ctnnb1*$^{fl/fl}$ mutants (N), *Dkk1*/*Krm1* triple transgenics (P) and *Krt15-CrePR1*

Wls$^{fl/fl}$ mutants (T) showed some evidence of inflammation compared with controls (M,O,S), but this was much less severe than in *Krt14-CreER Ctnnb1*$^{fl/fl}$ and *Krt5-rtTA tetO-Cre Wls*$^{fl/fl}$ mutants. Scale bars: 20μm (A-D); 500nm (E-J); 100μm (K-T). (U) Targeting scheme for insertion of *CreERT2tdT* cDNA into the endogenous *Axin2* locus. 7.2kb of BAC DNA containing *Axin2* genomic sequences was introduced into recombineering vector PL253 (Liu et al., 2003). *CreERT2* cDNA was fused with cytoplasmic tandem dimer Tomato (*tdT*) cDNA and a human growth hormone intron and polyA+ site and inserted into targeting vector PL451 (Liu et al., 2003). The fusion sequences were inserted into the PL253-*Axin2* construct downstream of the translation initiation codon using standard recombineering techniques (Liu et al., 2003), to generate a targeting vector. This was used for recombination in mouse ES cells to generate the *Axin2-CreERT2tdT* insertional mutation. Targeted ES cells were identified by Southern blot analysis of genomic DNA cut with *NcoI* and hybridized with the indicated 5' probe (identifies restriction fragments of 5.7kb and 8.7kb in the targeted and wild-type loci, respectively), and cut with *Xba1* and hybridized with 3' probe (identifies restriction fragments of 5.6kb and 8.8kb in the targeted and wild-type loci, respectively).

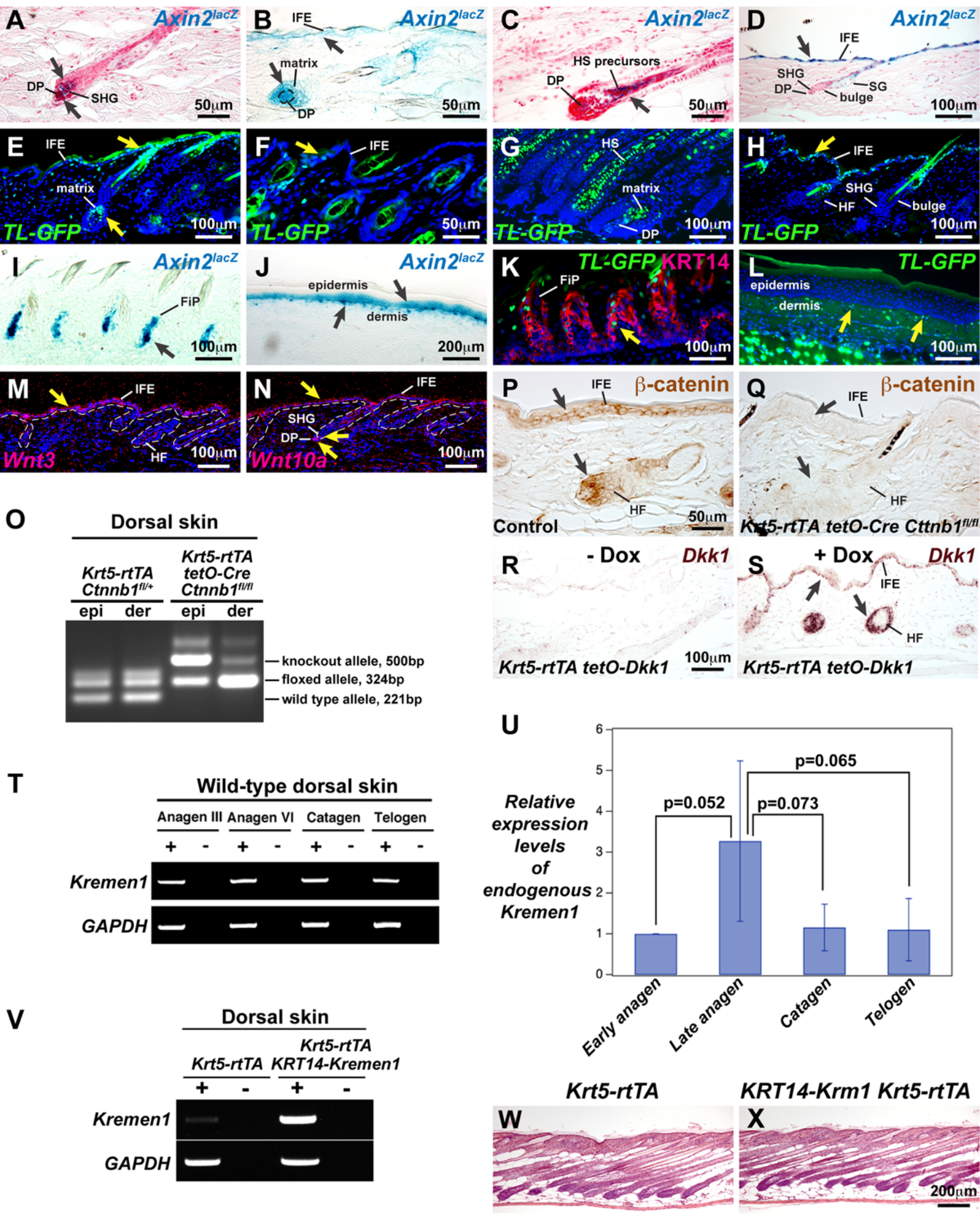
A
Axin2lacZ
DP
SHG
50μm
B
IFE
Axin2lacZ
matrix
DP
50μm
C
Axin2lacZ
HS precursors
DP
50μm
D
Axin2lacZ
IFE
SHG
DP
SG
bulge
100μm
E
IFE
matrix
TL-GFP
100μm
F
IFE
TL-GFP
50μm
G
HS
matrix
DP
TL-GFP
100μm
H
IFE
SHG
HF
bulge
TL-GFP
100μm
I
Axin2lacZ
FiP
100μm
J
Axin2lacZ
epidermis
dermis
200μm
K
TL-GFP KRT14
FiP
100μm
L
TL-GFP
epidermis
dermis
100μm
M
IFE
HF
Wnt3
100μm
N
IFE
SHG
DP
Wnt10a
100μm
P
IFE
β-catenin
HF
Control
50μm
Q
IFE
β-catenin
HF
Krt5-rtTA tetO-Cre Cttnb1fl/fl
O
Dorsal skin
Krt5-rtTA Ctnnb1fl/+
Krt5-rtTA tetO-Cre Ctnnb1fl/fl
epi
der
epi
der
knockout allele, 500bp
floxed allele, 324bp
wild type allele, 221bp
R
- Dox
Dkk1
Krt5-rtTA tetO-Dkk1
100μm
S
+ Dox
Dkk1
IFE
HF
Krt5-rtTA tetO-Dkk1
T
Wild-type dorsal skin
Anagen III
Anagen VI
Catagen
Telogen
+ - + - + - + -
Kremen1
GAPDH
U
Relative expression levels of endogenous Kremen1
0
1
2
3
4
5
6
p=0.052
p=0.073
p=0.065
Early anagen
Late anagen
Catagen
Telogen
V
Dorsal skin
Krt5-rtTA
Krt5-rtTA KRT14-Kremen1
+ - + -
Kremen1
GAPDH
Krt5-rtTA
KRT14-Krm1 Krt5-rtTA
W
X
200μm

Figure S1

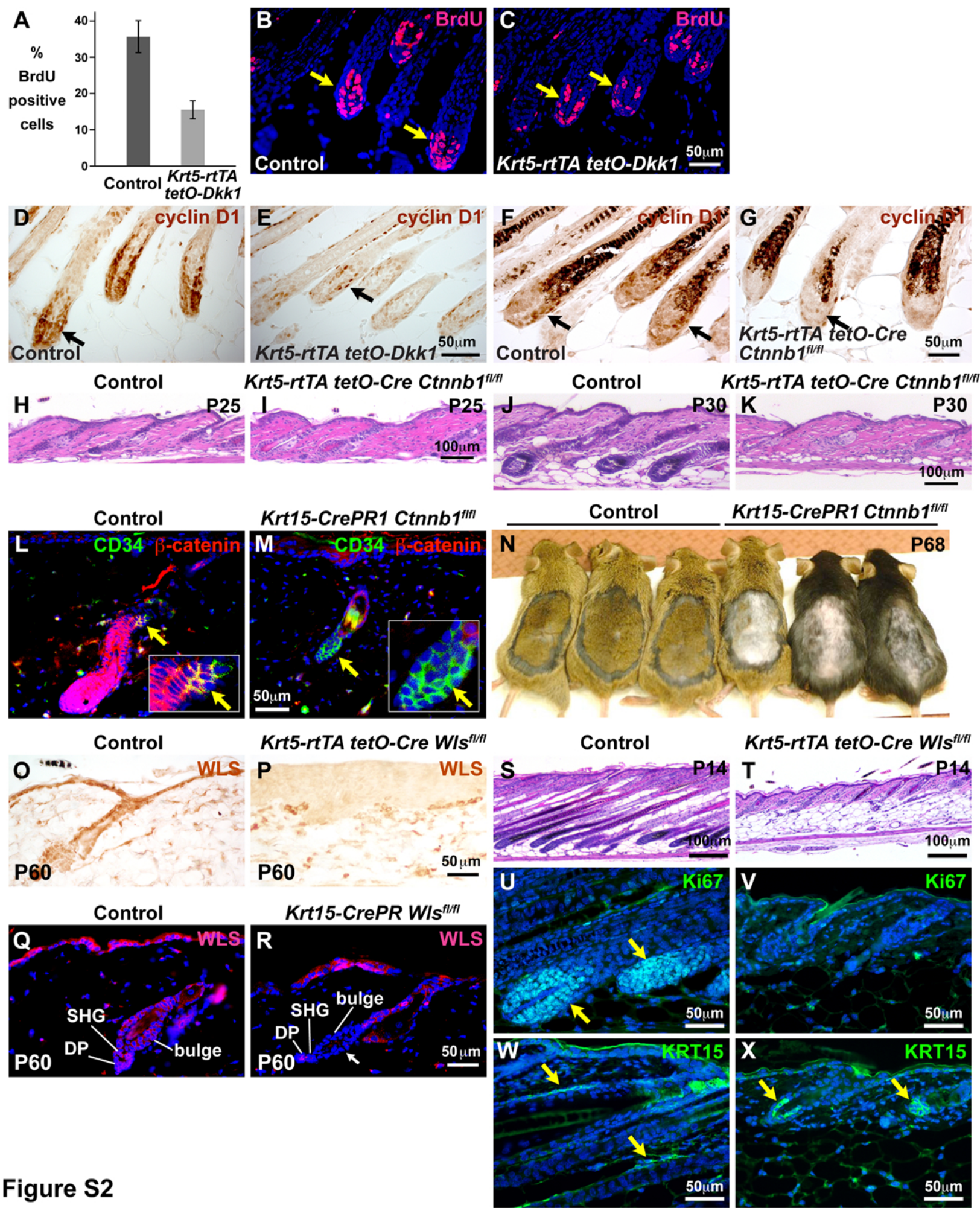
A
% BrdU positive cells
40
30
20
10
0
Control
Krt5-rtTA tetO-Dkk1
B
BrdU
Control
C
BrdU
Krt5-rtTA tetO-Dkk1
50μm
D
cyclin D1
Control
E
cyclin D1
Krt5-rtTA tetO-Dkk1
50μm
F
cyclin D1
Control
G
cyclin D1
Krt5-rtTA tetO-Cre Ctnnb1fl/fl
50μm
Control
Krt5-rtTA tetO-Cre Ctnnb1fl/fl
H
P25
I
P25
100μm
Control
Krt5-rtTA tetO-Cre Ctnnb1fl/fl
J
P30
K
P30
100μm
Control
Krt15-CrePR1 Ctnnb1fl/fl
L
CD34 β-catenin
M
CD34 β-catenin
50μm
Control
Krt15-CrePR1 Ctnnb1fl/fl
N
P68
Control
Krt5-rtTA tetO-Cre Wlsfl/fl
O
WLS
P60
P
WLS
P60
50 μm
Control
Krt5-rtTA tetO-Cre Wlsfl/fl
S
P14
100μm
T
P14
100μm
Control
Krt15-CrePR Wlsfl/fl
Q
WLS
SHG
DP
bulge
P60
R
WLS
SHG
DP
bulge
P60
50 μm
U
Ki67
50μm
V
Ki67
50μm
W
KRT15
50μm
X
KRT15
50μm

Figure S2

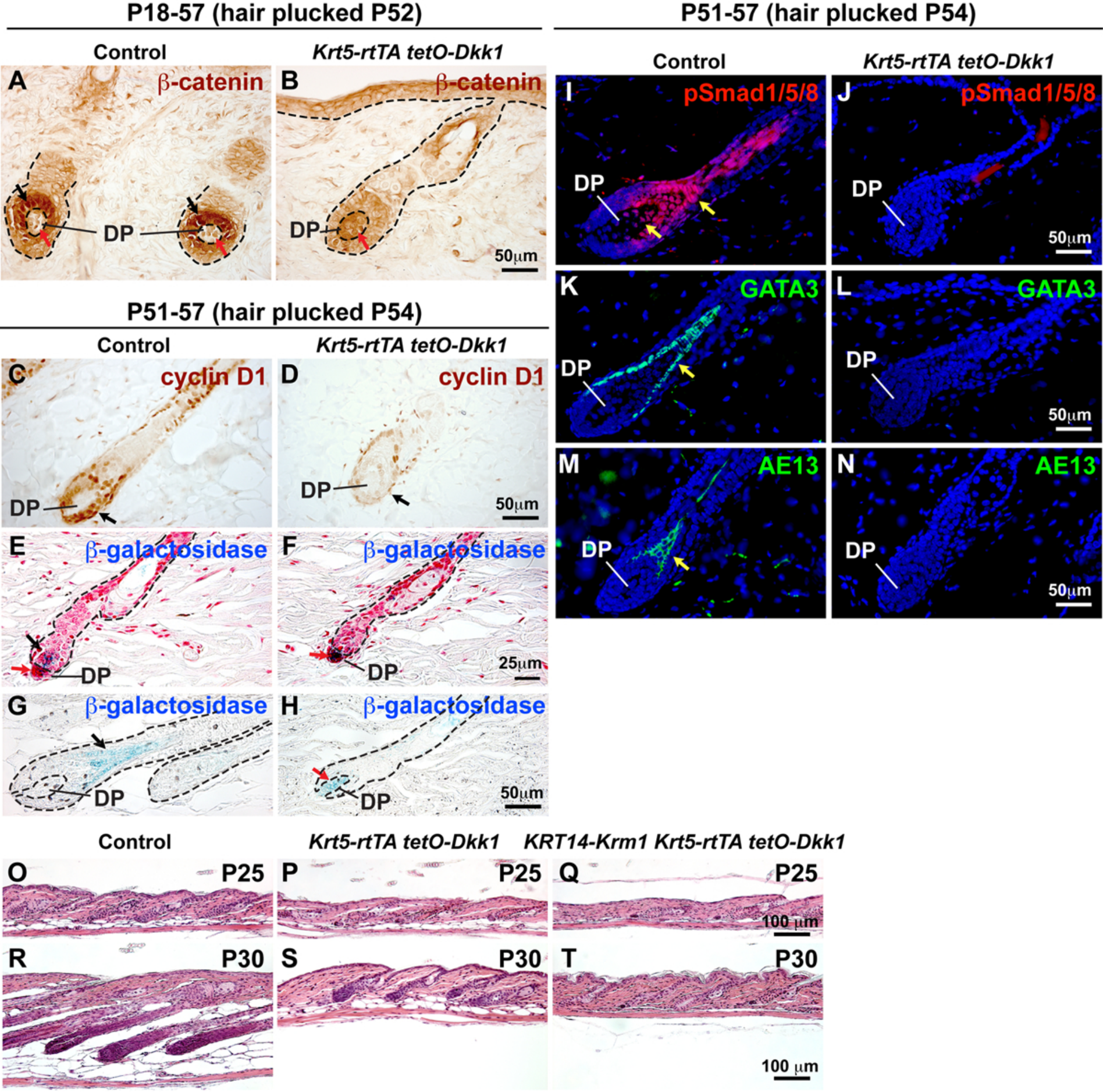
P18-57 (hair plucked P52)
Control
Krt5-rtTA tetO-Dkk1
A
β-catenin
DP
B
β-catenin
DP
50μm
P51-57 (hair plucked P54)
Control
Krt5-rtTA tetO-Dkk1
I
pSmad1/5/8
DP
J
pSmad1/5/8
DP
50μm
K
GATA3
DP
L
GATA3
DP
50μm
M
AE13
DP
N
AE13
DP
50μm
P51-57 (hair plucked P54)
Control
Krt5-rtTA tetO-Dkk1
C
cyclin D1
DP
D
cyclin D1
DP
50μm
E
β-galactosidase
DP
F
β-galactosidase
DP
25μm
G
β-galactosidase
DP
H
β-galactosidase
DP
50μm
Control
Krt5-rtTA tetO-Dkk1
KRT14-Krm1 Krt5-rtTA tetO-Dkk1
O
P25
P
P25
Q
P25
100 μm
R
P30
S
P30
T
P30
100 μm

Figure S3

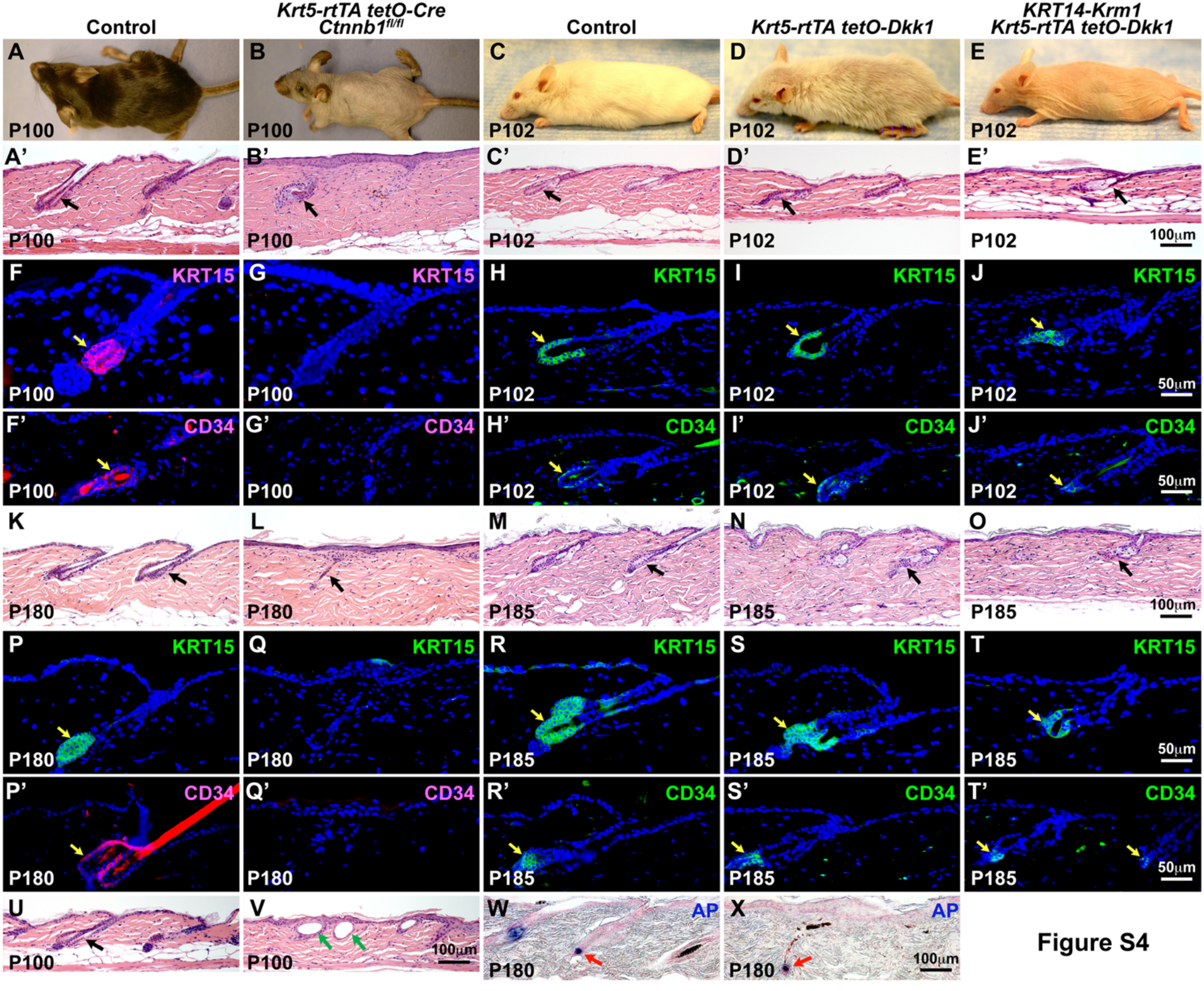
Control
Krt5-rtTA tetO-Cre
Ctnnb1fl/fl
Control
Krt5-rtTA tetO-Dkk1
KRT14-Krm1
Krt5-rtTA tetO-Dkk1
A
P100
B
P100
C
P102
D
P102
E
P102
A'
P100
B'
P100
C'
P102
D'
P102
E'
P102
100μm
F
KRT15
P100
G
KRT15
P100
H
KRT15
P102
I
KRT15
P102
J
KRT15
P102
50μm
F'
CD34
P100
G'
CD34
P100
H'
CD34
P102
I'
CD34
P102
J'
CD34
P102
50μm
K
P180
L
P180
M
P185
N
P185
O
P185
100μm
P
KRT15
P180
Q
KRT15
P180
R
KRT15
P185
S
KRT15
P185
T
KRT15
P185
50μm
P'
CD34
P180
Q'
CD34
P180
R'
CD34
P185
S'
CD34
P185
T'
CD34
P185
50μm
U
P100
V
P100
100μm
W
AP
P180
X
AP
P180
100μm

Figure S4

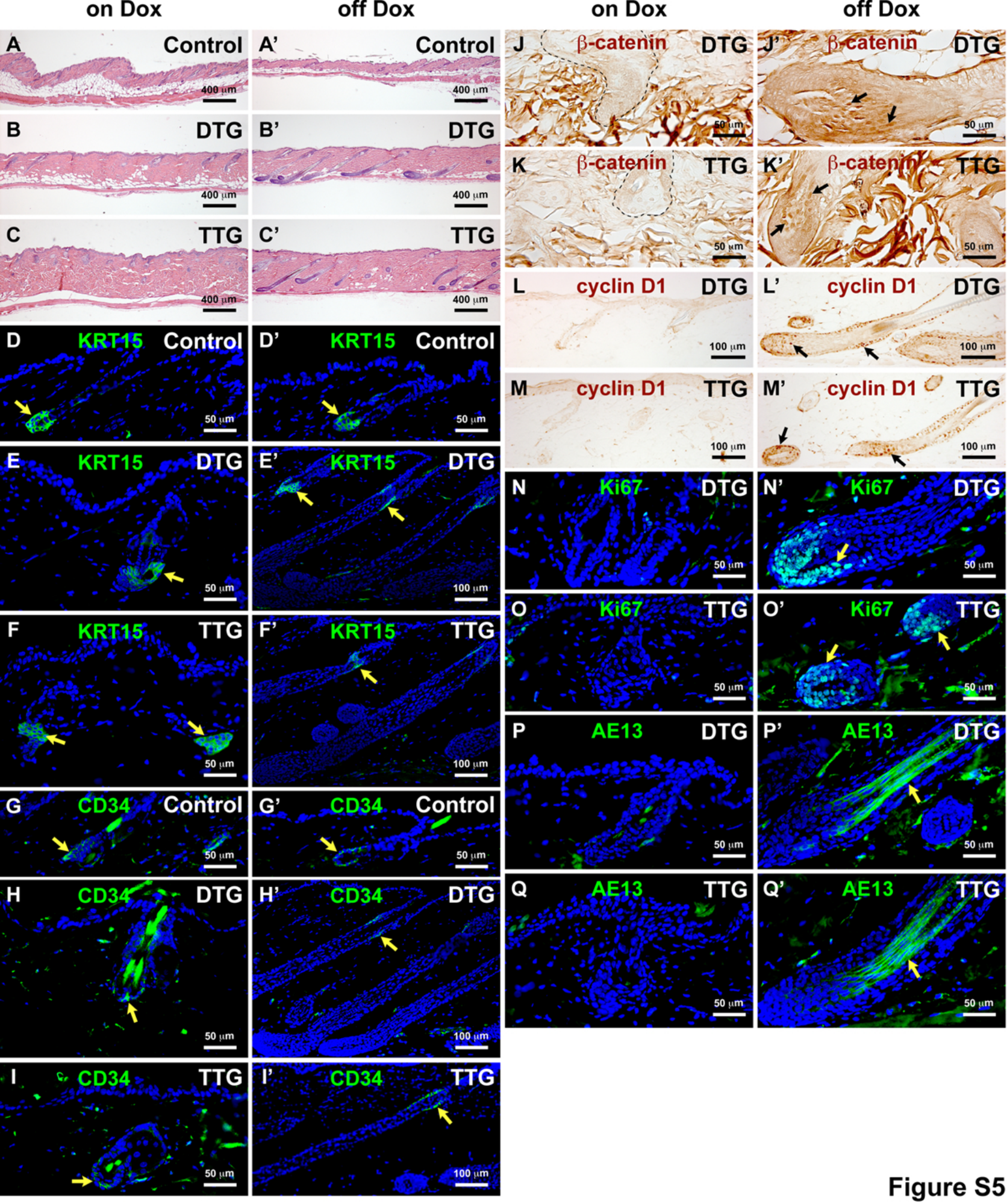
on Dox
off Dox
on Dox
off Dox
A
Control
A'
Control
B
DTG
B'
DTG
C
TTG
C'
TTG
400 μm
D
KRT15
Control
D'
KRT15
Control
E
KRT15
DTG
E'
KRT15
DTG
F
KRT15
TTG
F'
KRT15
TTG
G
CD34
Control
G'
CD34
Control
H
CD34
DTG
H'
CD34
DTG
I
CD34
TTG
I'
CD34
TTG
50 μm
100 μm
J
β-catenin
DTG
J'
β-catenin
DTG
K
β-catenin
TTG
K'
β-catenin
TTG
L
cyclin D1
DTG
L'
cyclin D1
DTG
M
cyclin D1
TTG
M'
cyclin D1
TTG
N
Ki67
DTG
N'
Ki67
DTG
O
Ki67
TTG
O'
Ki67
TTG
P
AE13
DTG
P'
AE13
DTG
Q
AE13
TTG
Q'
AE13
TTG

Figure S5

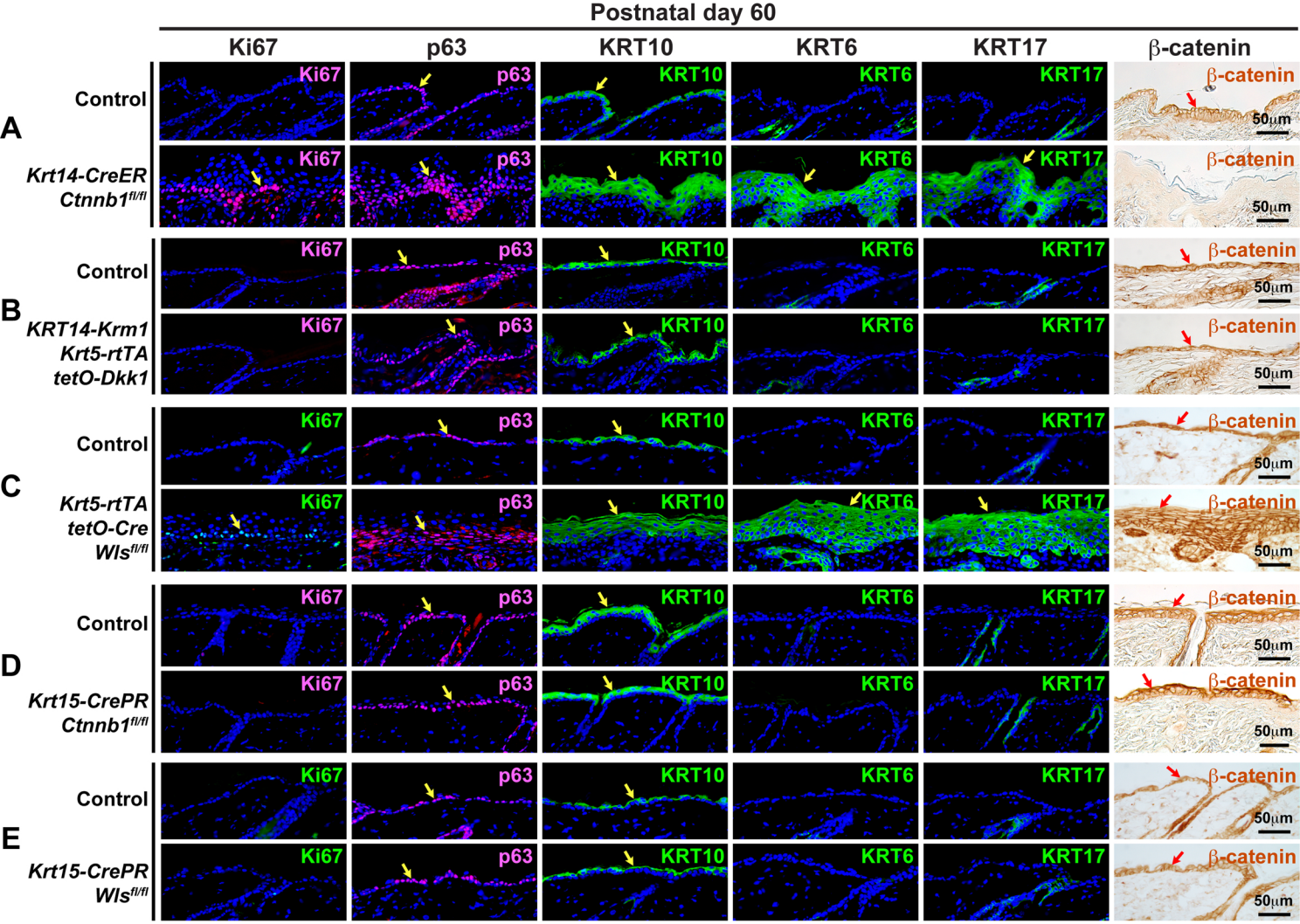
Postnatal day 60
Ki67
p63
KRT10
KRT6
KRT17
β-catenin
A
Control
Krt14-CreER
Ctnnb1fl/fl
B
Control
KRT14-Krm1
Krt5-rtTA
tetO-Dkk1
C
Control
Krt5-rtTA
tetO-Cre
Wlsfl/fl
D
Control
Krt15-CrePR
Ctnnb1fl/fl
E
Control
Krt15-CrePR
Wlsfl/fl
50μm

Figure S6

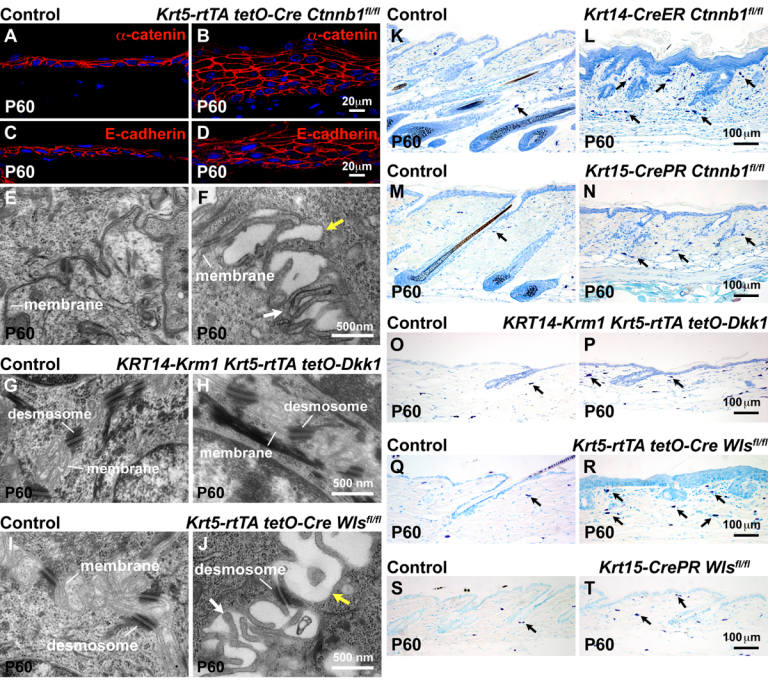
Control
Krt5-rtTA tetO-Cre Ctnnb1fl/fl
A
α-catenin
P60
B
α-catenin
P60
20μm
C
E-cadherin
P60
D
E-cadherin
P60
20μm
E
membrane
P60
F
membrane
P60
500nm
Control
KRT14-Krm1 Krt5-rtTA tetO-Dkk1
G
desmosome
membrane
P60
H
desmosome
membrane
P60
500 nm
Control
Krt5-rtTA tetO-Cre Wlsfl/fl
I
membrane
desmosome
P60
J
desmosome
P60
500 nm
Control
Krt14-CreER Ctnnb1fl/fl
K
P60
L
P60
100 μm
Control
Krt15-CrePR Ctnnb1fl/fl
M
P60
N
P60
100 μm
Control
KRT14-Krm1 Krt5-rtTA tetO-Dkk1
O
P60
P
P60
100 μm
Control
Krt5-rtTA tetO-Cre Wlsfl/fl
Q
P60
R
P60
100 μm
Control
Krt15-CrePR Wlsfl/fl
S
P60
T
P60
100 μm

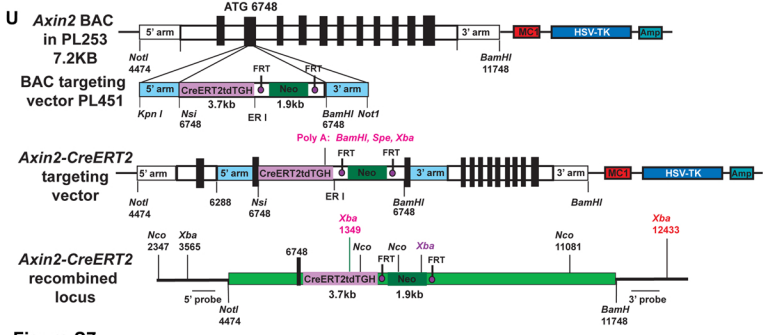
U
Axin2 BAC in PL253 7.2KB
ATG 6748
5' arm
3' arm
MC1
HSV-TK
Amp
NotI 4474
BamHI 11748
BAC targeting vector PL451
5' arm
CreERT2tdTGH
Neo
3' arm
FRT
FRT
3.7kb
1.9kb
Kpn I
Nsi 6748
ER I
BamHI 6748
Not1
Axin2-CreERT2 targeting vector
Poly A: BamHI, Spe, Xba
NotI 4474
6288
Nsi 6748
ER I
BamHI 6748
BamHI
Axin2-CreERT2 recombined locus
Nco 2347
Xba 3565
Xba 1349
6748
Nco
Nco
Xba
Nco 11081
Xba 12433
5' probe
NotI 4474
3.7kb
1.9kb
3' probe
BamH 11748

Figure S7

SUPPLEMENTAL EXPERIMENTAL PROCEDURES

Generation and breeding of mouse strains, transgene induction, depilation, skin biopsies, and genotyping

A *KRT14-Krm1* transgene, constructed by cloning full-length mouse *Krm1* cDNA (NM_032396) into a *KRT14* promoter vector (Saitou et al., 1995), was microinjected into fertilized eggs by the Transgenic and Chimeric Mouse Facility, University of Pennsylvania. *K14-Kremen1* transgene-expressing lines were generated from two founder mice and were grossly normal. Mice from one of these lines were crossed to *Krt5-rtTA tetO-Dkk1* mice to generate *Krt5-rtTA tetO-Dkk1 KRT14-Krm1* mice. *Krt5-rtTA tetO-Dkk1* mice were crossed to $Axin2^{lacZ}$ mice (Lustig et al., 2002) for several generations to generate *Krt5-rtTA tetO-Dkk1* $Axin2^{lacZ}$ mice. *Krt5-rtTA tetO-Cre* mice were crossed with $Ctnnb1^{fl/fl}$ mice or $Wls^{fl/fl}$ mice (Jackson Labs, Bar Harbor, ME, USA) for several generations to generate *Krt5-rtTA tetO-Cre* $Ctnnb1^{fl/fl}$ mice and *Krt5-rtTA tetO-Cre* $Wls^{fl/fl}$ mice. To induce expression of *Dkk1* or deletion of β-catenin or *Wls*, respectively, weaned mice or mothers of nursing pups were placed on chow containing 6g/kg doxycycline (Bio-Serv, Laurel, MD, USA). *Krt15-CrePR1* $Ctnnb1^{fl/fl}$ mice and *Krt15-CrePR1* $Wls^{fl/fl}$ mice were generated by crossing *Krt15-CrePR1* mice (Jackson Labs, Bar Harbor, Maine, USA) (Morris et al., 2004) with $Ctnnb1^{fl/fl}$ mice or $Wls^{fl/fl}$ mice for several generations. Deletion of β-catenin or *Wls* was induced by applying 1% mifepristone (Sigma-Aldrich Corp., St. Louis, MO) in ethanol daily to dorsal skin for 5-7 days after hair clipping. *KRT14-CreER* $Ctnnb1^{fl/fl}$ mice were generated by crossing *KRT14-CreER* mice (Jackson Labs) with $Ctnnb1^{fl/fl}$ mice for several generations. Transgene induction was performed by topical application of 2 mg 4OHT (Sigma) dissolved in acetone to dorsal skin after hair clipping.

For generation of *Axin2-CreERT2/tdTomato* (*Axin2-CreERT2/tdT*) mice, BAC clones bMQ-414F03, bMQ-311o15, bMQ313o15 and bMQ-226618 were obtained from the Sanger Institute (Hinxton, UK). 7.2kb of BAC DNA containing *Axin2* genomic sequences was introduced into recombineering vector PL253 (Liu et al., 2003) (Fig. S7U). *CreERT2* cDNA was fused with cytoplasmic tandem dimer Tomato (*tdT*) cDNA and a human growth hormone intron and polyA+ site and inserted into targeting vector PL451 (Liu et al., 2003). The fusion sequences were inserted into the PL253-*Axin2* construct downstream of the translation initiation codon using standard recombineering techniques (Liu et al., 2003), to generate a targeting vector. This was electroporated into mouse ES cells to generate the *Axin2-CreERT2tdT* insertional mutation by homologous recombination. Targeted ES cells were identified by Southern blot analysis of genomic DNA cut with *NcoI* and hybridized with a 5' probe that identifies restriction fragments of 5.7kb and 8.7kb in the targeted and wild-type loci, respectively, and cut with *Xba1* and hybridized with a 3' probe that identifies restriction fragments of 5.6kb and 8.8kb in the targeted and wild-type loci, respectively (Fig. S7U). Targeted ES cell clones were injected into fertilized mouse blastocysts that were implanted into pseudopregnant females. Resulting male chimeras were crossed to C57BL/6J mice (Jackson Laboratories) and Agouti offspring were genotyped for the *Axin2-CreERT2/tdT* allele by polymerase chain reaction (PCR) with wild-type forward primer: 5'-TCG GAT ACT TGA GAC GAG CAC CTC GCG GAT-3'; and mutant reverse primer: 5'-GTT ATT CAA CTT GCA CCA TGC CGC CCA CG-3'. Following removal of the Neo cassette by breeding to mice ubiquitously expressing FLP1 recombinase (Jackson Laboratories), *Axin2-CreERT2/tdT* mice were crossed for several generations to *Gt(ROSA)26Sor*$^{tm1(CAG-Brainbow2.1)Cle}$/J (*R26R-Confetti*), *Gt(ROSA)26Sor*$^{tm4(ACTB-tdTomato,-EGFP)Luo}$/J (*R26R*^{mTmG}) and/or *Ctnnb1*$^{fl/fl}$ mice (Jackson Labs, Bar Harbor, ME, USA). Tamoxifen was administered to

adult mice by intraperitoneal injection at 200mg/kg per day for 3 consecutive days to induce Cre activity.

For depilation experiments, mice were anesthetized with ketamine/xylazine and hair in a 1cm^2 area of mid-dorsal skin was manually plucked with forceps. Skin biopsies were taken from euthanized mice or under anesthesia. For reversibility experiments, mice maintained on doxycycline chow were anesthetized with ketamine/xylazine and a full thickness skin excision was made under sterile conditions using a 6mm biopsy punch according to an approved IACUC protocol. Mice were placed on regular chow, and a second biopsy was taken after euthanasia, 14-15 days after the first biopsy. Mice were genotyped by PCR analysis of genomic DNA extracted from tail biopsies. The Institutional Animal Care and Use Committee of the University of Pennsylvania approved all experimental procedures involving mice.

In situ hybridization, immunostaining, TEM and photomicrography

In situ hybridization methods and probes for *Dkk1*, *Wnt3*, and *Wnt10a* were as described previously (Andl et al., 2002; Reddy et al., 2001). For immunostaining, sections were microwave pretreated and incubated with primary antibodies against Ki67 (1:40), KRT6 (1:400) or KRT10 (1:500) (Covance, Princeton, New Jersey, USA); cytokeratin15 (1:50) (Vector Laboratories, Burlingame, CA, USA); GATA3 (HCG3-31) (1:100) or β-catenin (1:1000) (Sigma-Aldrich Corp., St. Louis, MO, USA); phospho-SMAD1,5,8 (1:50) or cyclin D1 (1:25) (Cell Signaling Technology, Danvers, MA, USA); AE13 (1:100) (Abcam); or BMP6 (1:50) (Santa Cruz Biotechnology, Inc., Santa Cruz, CA, USA); CD34 (1:50) (BD Biosciences, San Jose, CA, USA); p63 (1:100) (Thermo Scientific); KRT17 (1:5,000) (a gift from P. Coulombe). Immunoflurescence for α-catenin (1:1000) (BD Bioscience) and E-cadherin (1:200) (Invitrogen) was performed on frozen sections. Toluidine blue

staining was performed on paraffin sectioned skin using the NovaUltra Toluidine Blue Stain Kit (IHCWORLD). Images were captured using a Leica DM4000B microscope, Leica DC500 digital camera and Leica FireCam software version 1.4 (Leica Microsystems, Buffalo Grove, IL, USA). For TEM, tissue was fixed in 2% glutaraldehyde in 0.1% sodium cacodylate buffer, post-fixed in 1% osmium tetroxide, and embedded in Epoxy resin. Ultrathin sections were contrasted with double stains and examined with a FEITecnai-T12 transmission electron microscope.

SUPPLEMENTAL REFERENCES

Andl, T., Reddy, S.T., Gaddapara, T., and Millar, S.E. (2002). WNT Signals Are Required for the Initiation of Hair Follicle Development. Dev Cell *2*, 643-653.

Liu, P., Jenkins, N.A., and Copeland, N.G. (2003). A highly efficient recombineering-based method for generating conditional knockout mutations. Genome Res *13*, 476-484.

Lustig, B., Jerchow, B., Sachs, M., Weiler, S., Pietsch, T., Karsten, U., van de Wetering, M., Clevers, H., Schlag, P.M., Birchmeier, W.*, et al.* (2002). Negative feedback loop of Wnt signaling through upregulation of conductin/axin2 in colorectal and liver tumors. Mol Cell Biol *22*, 1184-1193.

Morris, R.J., Liu, Y., Marles, L., Yang, Z., Trempus, C., Li, S., Lin, J.S., Sawicki, J.A., and Cotsarelis, G. (2004). Capturing and profiling adult hair follicle stem cells. Nat Biotechnol *22*, 411-417.

Reddy, S., Andl, T., Bagasra, A., Lu, M.M., Epstein, D.J., Morrisey, E.E., and Millar, S.E. (2001). Characterization of Wnt gene expression in developing and postnatal hair follicles and identification of Wnt5a as a target of Sonic hedgehog in hair follicle morphogenesis. Mech Dev *107*, 69-82.